Int. J. Heat Mass Transfer. Vol. 22, pp. 919–927

0017-9310/79/0601-0919 $02.00/0

NATURAL CONVECTION IN HORIZONTAL SPACE BOUNDED BY TWO CONCENTRIC CYLINDERS WITH DIFFERENT END TEMPERATURES

ADRIAN BEJAN
Department of Mechanical Engineering, University of Colorado, Boulder, CO 80309, U.S.A.

and

CHANG-LIN TIEN
Department of Mechanical Engineering, University of California, Berkeley, CA 94720, U.S.A.

(*Received* 12 *May* 1978 *and in revised form* 21 *November* 1978)

Abstract—The gravity-induced flow in a long horizontal space of annular cross-section insulated laterally and with the two ends maintained at different temperatures was studied analytically. The velocity and temperature distribution in the central portion of the space was derived based on a perturbation analysis in the Rayleigh number. The Nusselt number for axial heat transfer was shown to depend on the Rayleigh number, the two geometric aspect ratios r_i/r_0 and L/r_0 (inner radius/outer radius and length/outer radius) plus the conducting properties of the two cylindrical walls. The analysis was performed for the case where the horizontal space is filled with incompressible fluid and the case where the space is filled with a porous material saturated with an incompressible fluid. The limit $r_i \to r_0$ was used finally to derive expressions for the flow and temperature fields between two vertical planes subjected to a net temperature difference in the horizontal direction parallel to the planes.

NOMENCLATURE

a_{-1}, a_1, constants, equation (23);
$b_{i,0}$, wall thickness [m];
c_{-1}, c_1, constants, equation (49);
$f_{u,v,T}$, functions, equations (51), (52) and (56–59);
$F_{u,v,w,T}$, functions, equations (25), (26), (29) and (36–38);
g, gravitational acceleration [m/s^2];
h, half-height of vertical walls, Fig. 5;
k, thermal conductivity of incompressible fluid or saturated porous medium;
$k_{i,0}$, thermal conductivity of cylindrical walls;
K, permeability [m^2];
K_1, K_2, constants, equations (17) and (46);
Nu, Nusselt number, equation (27);
P, pressure, equation (7);
Pr, Prandtl number, ν/α;
Q, axial heat transfer rate [W];
r, radial position, equation (4a);
$r_{i,0}$, radii of concentric cylinders;
$R_{i,0}$, wall thermal resistance parameter, equations (12a,b);
Ra, Rayleigh number, equations (9) and (42);
t, spacing between vertical walls [m];
T, temperature, equation (6);
ΔT, end-to-end temperature difference;
u,v,w, velocity components, equation (5) and Fig. 1;
x, horizontal (lateral) coordinate, equation (32) and Fig. 5;
y, vertical coordinate, equation (33) and Fig. 5;
z, axial coordinate, equation (4b) and Figs. 1 and 5;
$( )^*$, dimensional quantities;
∇^2, Laplacian operator in cylindrical coordinates,
$$\frac{\partial^2}{\partial r^2}+\frac{1}{r}\frac{\partial}{\partial r}+\frac{1}{r^2}\frac{\partial^2}{\partial \theta^2}+\frac{\partial^2}{\partial z^2}.$$

Greek symbols

α, thermal diffusivity of incompressible fluid or saturated porous medium [m^2/s];
β, coefficient of volumetric thermal expansion [K^{-1}];
δ, annulus thickness ratio, $(r_0-r_i)/r_0$;
θ, tangential direction, Fig. 1;
μ, viscosity [Kg/(ms)];
ν, kinematic viscosity [m^2/s];
ρ, radii ratio r_i/r_0;
$\tilde{\rho}$, density [Kg/m^3].

Subscripts

i, inner radius;
o, outer radius;
0,1,2, zeroth, first, second order approximation.

INTRODUCTION

NATURAL convection heat transfer in insulated horizontal conduits subjected to an end-to-end temperature difference has only recently come into focus. The different end temperatures produce a horizontal counterflow pattern in which colder fluid

flows along the bottom of the conduit and warmer fluid flows in the opposite direction along the top. Hong [1] studied numerically the effect of this counterflow on the temperature distribution and concentration of thermal stresses in the conducting wall of round pipes. Bejan and Tien [2] studied the same phenomenon analytically by means of a perturbation analysis valid for small Rayleigh numbers. They showed that as the Rayleigh number increases the axial counterflow in round pipes is also accompanied by a secondary flow composed of spiraling eddies in each quadrant of the pipe cross-section. A similar flow pattern prevails in a horizontal cylinder filled with a porous medium subjected to an end-to-end temperature difference [3].

In an earlier three-paper sequence, Cormack *et al.* [4, 5] and Imberger [6] studied the natural convection in a slender two-dimensional cavity with differently heated end walls. Their work was aimed at describing the spreading of thermal polution through estuaries and other shallow waters. Bejan and Tien [7] proposed an integral method to account for the flow in the vicinity of open or closed ends of parallel-plate horizontal channels with different end temperatures. Bejan and Tien applied the same technique to the study of natural convection through horizontal porous layers with permeable or impermeable end-walls maintained at different temperatures [3].

The objective of this work is to study analytically the heat-transfer mechanism by natural convection through a long conduit of annular cross-section, subjected to an end-to-end temperature difference. This free connection phenomenon has applications in the study of thermal stresses in the walls of horizontal conduits of annular cross-section. Also, the horizontal heat leak induced by the free connection mechanism is a critical parameter in the design of cryogenic systems.

In the first part of this article we consider the case of an incompressible fluid bounded by two horizontal cylinders. A perturbation analysis in the Rayleigh number as a small parameter leads to a set of asymptotic expressions for the velocity and the temperature field in the annular cross-section. The Nusselt number for axial heat transfer is estimated, showing the effect of radii ratio r_0/r_i and the effect of thermal conduction through the two cylindrical walls. The limit $r_i \to r_0$ is finally used to derive the natural convection pattern in a parallelepiped with the height h much greater than the horizontal thickness t.

The second part of this paper deals with natural convection through a porous medium bounded by two horizontal cylinders. Analytically, the problem is similar to the one treated in the first part. The velocity and temperature distributions and the Nusselt number for axial heat transfer through the porous medium are derived based on a perturbation analysis. Applying the limit $r_i \to r_0$, this solution is used to derive the horizontal convective pattern in a porous layer of rectangular cross-section with $h \gg t$.

SPACE FILLED WITH INCOMPRESSIBLE FLUID

The annular space and its dimensions are shown on Fig. 1. The horizontal cylindrical surfaces are adiabatic. However, each cylinder is modeled as a conducting sheet of zero thickness, capable of conducting heat in the tangential and axial directions. A net temperature difference ΔT is maintained across the two ends of the annular space.

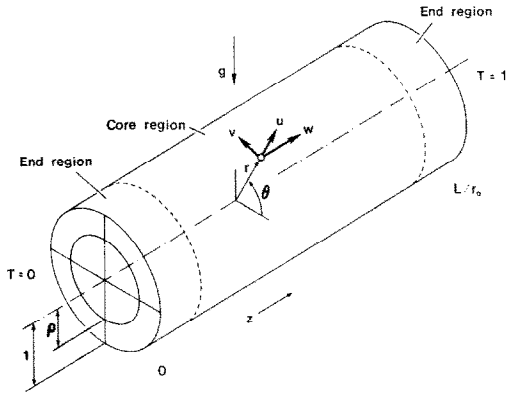

FIG. 1. Horizontal space bounded by concentric horizontal cylinders with different end temperatures.

(a) *Formulation of the problem*

The equations governing conservation of mass, momentum and energy in the steady state are

$$\frac{u}{r}+\frac{\partial u}{\partial r}+\frac{1}{r}\frac{\partial v}{\partial \theta}+\frac{\partial w}{\partial z}=0, \tag{1}$$

$$\frac{1}{Pr}\left(u\frac{\partial u}{\partial r}+\frac{v}{r}\frac{\partial u}{\partial \theta}+w\frac{\partial u}{\partial z}-\frac{v^2}{r}\right) = -\frac{gr_0^3}{\alpha\nu}\sin\theta+Ra\sin\theta T-\frac{\partial P}{\partial r} +\nabla^2 u-\frac{u}{r^2}-\frac{2}{r^2}\frac{\partial v}{\partial \theta}, \tag{2a}$$

$$\frac{1}{Pr}\left(u\frac{\partial v}{\partial r}+\frac{v}{r}\frac{\partial v}{\partial \theta}+w\frac{\partial v}{\partial z}+\frac{uv}{r}\right) = -\frac{gr_0^3}{\alpha\nu}\cos\theta+Ra\cos\theta T-\frac{1}{r}\frac{\partial P}{\partial \theta} +\nabla^2 v+\frac{2}{r^2}\frac{\partial u}{\partial \theta}-\frac{v}{r^2}, \tag{2b}$$

$$\frac{1}{Pr}\left(u\frac{\partial w}{\partial r}+\frac{v}{r}\frac{\partial w}{\partial \theta}+w\frac{\partial w}{\partial z}\right)=-\frac{\partial P}{\partial z}+\nabla^2 w, \tag{2c}$$

$$u\frac{\partial T}{\partial r}+\frac{v}{r}\frac{\partial T}{\partial \theta}+w\frac{\partial T}{\partial z}=\nabla^2 T. \tag{3}$$

The cylindrical coordinate system r,θ,z is shown in Fig. 1. Equations (1)–(3) have been put into non-dimensional form by defining the following dimensionless variables.

$$(r, z)=(r, z)^*/r_o, \tag{4a,b}$$

$$(u, v, w)=(u, v, w)^* r_o/\alpha, \tag{5a,b,c}$$

$$T = T^*/\Delta T, \tag{6}$$

$$P = P^* r_o^2/(\alpha\mu). \tag{7}$$

The asterisks denote the dimensional quantities of this problem. The temperature difference T^* was assumed zero at $z = 0$. The fluid filling the annular space is incompressible, subject to the Boussinesq approximation by which density differences are due solely to temperature differences

$$\tilde{\rho} = \tilde{\rho}_0[1 - \beta(T^* - T_o^*)], \tag{8}$$

where subscript 0 denotes the properties of a reference state. The convective flow intensity is governed by the Rayleigh number defined as

$$Ra = \frac{g\beta r_o^3 \Delta T}{\alpha\nu}. \tag{9}$$

We are interested in determining the velocity field (u,v,w) and the temperature field T by solving equations (1)–(3) subject to velocity and temperature boundary conditions along the walls of the annular space. In the radial direction, the boundary conditions are

$$(u,v,w) = 0, \quad \text{at} \quad r = \rho, 1, \tag{10a,b}$$

$$\frac{\partial^2 T}{\partial z^2} + \frac{1}{\rho^2}\frac{\partial^2 T}{\partial \theta^2} = -R_i \frac{\partial T}{\partial r}, \quad \text{at } r = \rho, \tag{11a}$$

$$\frac{\partial^2 T}{\partial z^2} + \frac{\partial^2 T}{\partial \theta^2} = R_o \frac{\partial T}{\partial r}, \quad \text{at} \quad r = 1, \tag{11b}$$

where $\rho = r_i/r_o$. Equations (11a,b) are the temperature boundary conditions around the concentric cylindrical surfaces. Parameters R_i, R_o are the dimensionless thermal resistances of the two walls,

$$R_{i,o} = \frac{kr_o^2}{(kb)_{i,o}}, \tag{12a,b}$$

where $k_{i,o}$ is the wall conductivity and $b_{i,o}$ the wall radial thickness assumed much smaller than either r_i or r_o.

As shown in all previous studies [1–7], in long horizontal spaces with different end temperatures the velocity field is independent of axial position over the central portion of the space (the core region). The effect of the two end-walls on the velocity field is restricted to two small segments of the long horizontal space located near the two ends. In what follows, we seek expressions for u,v,w,T in the core region only. The end-wall effect on the natural counterflow through the annular space will be discussed in the closing section of this paper.

(b) *The perturbation method*

An analytical solution to equations (1)–(3) is obtained by first eliminating the pressure terms among the three momentum equations (2a,b,c). This is done by differentiating (2a) with respect to θ and z and combining the results with the partial derivatives of equations (2b,c) with respect to r. The resulting momentum conditions are

$$\begin{aligned}
&\frac{\partial}{\partial\theta}\left[\frac{1}{Pr}\left(u\frac{\partial u}{\partial r} + \frac{v}{r}\frac{\partial u}{\partial\theta} + w\frac{\partial u}{\partial z} - \frac{v^2}{r}\right)\right. \\
&\quad \left. - \nabla^2 u + \frac{u}{r^2} + \frac{2}{r^2}\frac{\partial v}{\partial\theta}\right] \\
&\quad - \frac{\partial}{\partial r}\left\{r\left[\frac{1}{Pr}\left(u\frac{\partial v}{\partial r} + \frac{v}{r}\frac{\partial v}{\partial\theta} + w\frac{\partial v}{\partial z} + \frac{uv}{r}\right)\right.\right. \\
&\quad \left.\left. - \nabla^2 v + \frac{v}{r^2} - \frac{2}{r^2}\frac{\partial u}{\partial\theta}\right]\right\} \\
&\quad = Ra\left(\sin\theta\frac{\partial T}{\partial\theta} - r\cos\theta\frac{\partial T}{\partial r}\right)
\end{aligned} \tag{13}$$

$$\begin{aligned}
&\frac{\partial}{\partial r}\left[\nabla^2 w - \frac{1}{Pr}\left(u\frac{\partial w}{\partial r} + \frac{v}{r}\frac{\partial w}{\partial\theta} + w\frac{\partial w}{\partial z}\right)\right] \\
&\quad - \frac{\partial}{\partial z}\left[\nabla^2 u - \frac{u}{r^2} - \frac{2}{r^2}\frac{\partial v}{\partial\theta} - \frac{1}{Pr}\right. \\
&\quad \left.\times\left(u\frac{\partial u}{\partial r} + \frac{v}{r}\frac{\partial u}{\partial\theta} + w\frac{\partial u}{\partial z} - \frac{v^2}{r}\right)\right] \\
&\quad = Ra\sin\theta\frac{\partial T}{\partial z}.
\end{aligned} \tag{14}$$

The perturbation method consists of developing u,v,w,T in power series in the Rayleigh number,

$$\begin{aligned}
(u,v,w,T) = (u,v,w,T)_0 + Ra(u,v,w,T)_1 \\
+ Ra^2(u,v,w,T)_2 + \ldots.
\end{aligned} \tag{15}$$

By introducing expressions (15) into equations (1), (13), (14) and (3) and identifying the coefficients of each power of Ra leads to an infinite set of equations which can be solved analytically. The method of solution for an annular space is identical to the one employed by Bejan and Tien [2] in analyzing the natural counterflow through long horizontal pipes. In fact, the round pipe solution corresponds to the special case $\rho = 0$ of the more general solution developed below.

The zeroth order approximation to the velocity and temperature field describes the state of solid body conduction,

$$(u,v,z)_0 = 0, \tag{16}$$

$$T_0 = K_1 z + K_2. \tag{17}$$

If $Ra = 0$, constants K_1, K_2 are determined from the end temperature conditions $T_0(0) = 0$ and $T_0(L/r_o) = 1$ to yield

$$K_1 = r_o/L, \quad K_2 = 0. \tag{18}$$

The first order approximation is

$$(u,v)_1 = 0, \tag{19}$$

plus two equations for w_1 and T_1.

$$\frac{\partial}{\partial r}(\nabla^2 w_1) = K_1 \sin\theta, \tag{20}$$

$$\nabla^2 T_1 = K_1 w_1. \tag{21}$$

The solution to equations (20) and (21) is straightforward [2] and, for brevity, the details are omitted. The resulting first order temperature and axial velocity distributions are

$$w_1 = \tfrac{1}{8}K_1 \sin\theta\left[\rho^2\frac{1}{r} - (1+\rho^2)r + r^3\right], \quad (22)$$

$$T_1 = \tfrac{1}{8}K_1^2 \sin\theta\left[a_{-1}\frac{1}{r} + a_1 r + \tfrac{1}{2}\rho^2 r\ln r - \tfrac{1}{8}(1+\rho^2)r^3 + \tfrac{1}{24}r^5\right]. \quad (23)$$

Coefficients a_{-1}, a_1 represent complex algebraic expressions in ρ, R_i, R_o determined from substituting equation (23) into the temperature boundary conditions (11a,b).

The first order approximation to the velocity field reveals a horizontal counterflow caused by the different end temperatures. Figure 2 shows a series of axial velocity profiles along the vertical diameter of the circular cross-section for a range of values of ρ.

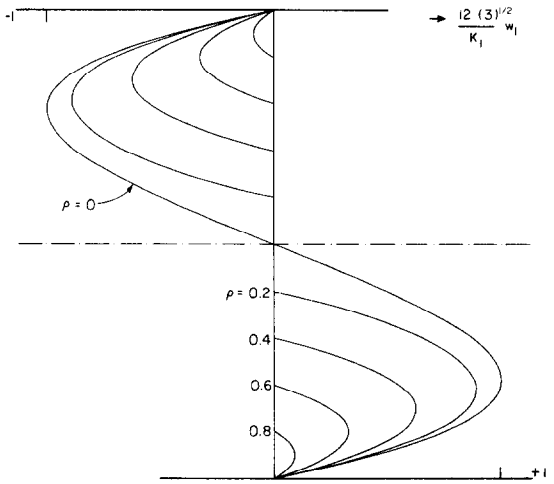

FIG. 2. Axial velocity distribution along a vertical diameter in the core region.

As the radii ratio approaches unity the axial counterflow decreases rapidly. The first order correction to the temperature field, T_1, is symmetric about the horizontal diameter of the annulus. Warmer fluid occupies the top half of the annular cross-section, flowing towards the cold end. Figure 3 shows the temperature distribution in the first quadrant for different ratios ρ in two extreme cases. The left column illustrates the case where both cylindrical surfaces are insulated, i.e. too thin to conduct heat appreciably (R_i, $R_o \to \infty$). The right column corresponds to the opposite case in which the two walls are infinitely conducting (R_i, $R_o = 0$). Figure 3 shows how increasing the radii ratio ρ and/or reducing the thermal resistance of the two walls has the effect of equalizing the fluid temperature in the cross-section, thus quenching the axial counterflow pattern.

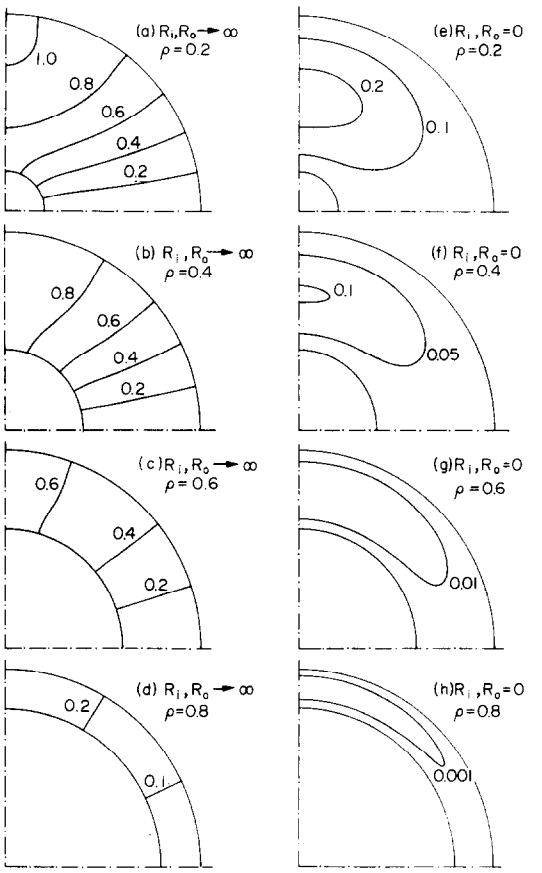

FIG. 3. Temperature distribution over the annulus in the core region. The numbers on the figure indicate the value of $96T_1/K_1^2$.

We also notice that the isotherms of Fig. 3 are not horizontal. In fact, at a constant height, the regions closer to the vertical diameter are warmer than the regions neighboring the outer wall. The relative temperature difference gives rise to an eddy in each quadrant, clockwise in the first quadrant shown in Fig. 3. This secondary flow can be determined analytically by carrying out the perturbation analysis beyond the first order correction, equations (19), (22) and (23). The second order correction has the form

$$(w, T)_2 = 0, \quad (24a,b)$$

$$u_2 = K_1^2 \cos 2\theta F_u(r), \quad (25)$$

$$v_2 = K_1^2 \sin 2\theta F_v(r), \quad (26)$$

where functions $F_u(r)$ and $F_v(r)$ are determined by solving the two equations (1) and (13).

(c) *Axial heat-transfer rate*

The purpose of the perturbation analysis presented above is to permit estimation of the Nusselt number for axial heat transport through the annular space. If Q is the net axial heat-transfer rate in the negative z direction, the Nusselt number can be defined as

$$Nu = \frac{Q}{\pi(1-\rho^2)r_0 k\Delta T}. \quad (27)$$

An energy flux analysis across any annular cross-section in the core region yields

$$Nu = \frac{1}{\pi(1-\rho^2)} \int_0^{2\pi} \int_0^1 \left(\frac{\partial T}{\partial z} - wT \right) r \, dr \, d\theta. \quad (28)$$

Expression (28) can now be evaluated using the perturbation solution for w and T,

$$Nu = K_1 - \frac{K_1^3 Ra^2}{64(1-\rho^2)} \int_\rho^1 F_w(r) F_T(r) r \, dr, \quad (29)$$

where F_w and F_T stand for two functions describing the radial variation of w_1 and T_1, equations (22) and (23). Since the secondary components w_2 and T_2 are zero, equations (24a,b), their contribution to axial heat transport is zero. The integral appearing in the convection term of expression (29) is negative since, for a given r, F_w and F_T have opposite sign (see Figs. 2 and 3).

The convection contribution to the Nusselt number depends on ρ, R_i and R_o; however, the complete expression showing this dependence is too lengthy to be reproduced here. We evaluated the Nusselt number in four limiting cases summarized on Fig. 4. The top curve shown in the figure corresponds to the case where both cylindrical walls are adiabatic (R_i, $R_o \to \infty$). If, in addition, ρ equals zero, expression (29) is greatly simplified,

$$Nu = K_1 + \frac{K_1^3 Ra^2}{23\,040}. \quad (30)$$

Equation (30) serves as reference to the Nu curves of Fig. 4 and is identical to the Nusselt number result obtained by Bejan and Tien [2] for horizontal adiabatic pipes with different end temperatures. The bottom curve of Fig. 4 shows the value of 23 040 $(Nu - K_1)/(K_1^3 Ra^2)$ for annular spaces bounded by two isothermal cylinders. The two intermediate curves correspond to the case in which one of the cylinders is adiabatic and the other is isothermal.

The convective part of the Nusselt number decreases sharply as the radii ratio approaches unity (see Fig. 4). The sharp decrease is due to the fact that, simultaneously, the axial velocity approaches zero and the temperature becomes isothermal over the cross-section. The heat-transfer rate is also reduced as one or both walls become more conducting. The two intermediate curves approach one another when $\rho \to 1$ since, in this limit, it makes little or no difference if the adiabatic wall is on the outside or on the inside boundary of the annular cross-section.

(d) *Horizontal counterflow between two vertical plates*

As the difference $t = r_o - r_i$ becomes much smaller than r_o, the two regions located in the vicinity of $\theta = 0$ and $\theta = \pi$ in the annular space of Fig. 1 resemble the space formed between two tall vertical plates, with the edges $z^* = 0$, L kept at different temperatures. The velocity and temperature distribution between the two vertical walls with corrections up to terms of Ra^2 can be derived immediately based on the perturbation solution obtained previously. For instance, applying the calculus of limits as $\rho \to 1$, the axial velocity becomes

$$w = -\tfrac{1}{2} K_1 Ra y x(\delta - x), \quad (31)$$

where

$$x = 1 - r, \quad (32)$$

$$y = \theta \cong \sin\theta, \quad (33)$$

$$\delta = t/h. \quad (34)$$

Everywhere in expressions (31)–(34), the half-height h replaces r_0 used as length scaling factor until now. We find that at any y the axial velocity profile is parabolic. The axial velocity is zero over the horizontal midplane of the box formed by the two vertical walls. If

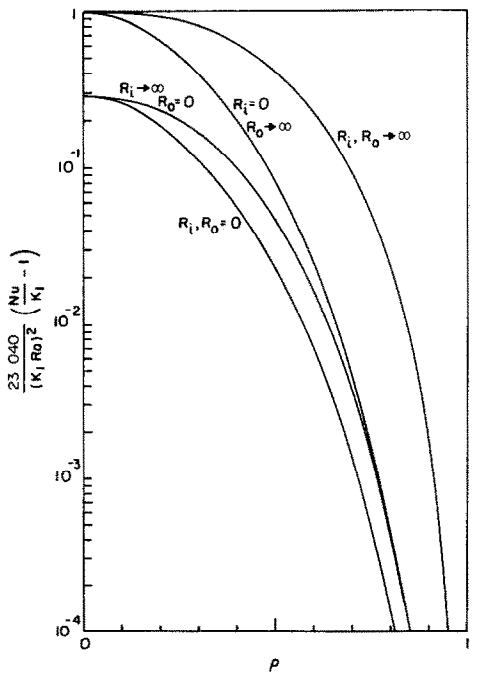

FIG. 4. Nusselt number vs radii ratio ρ for horizontal annular space filled with incompressible fluid.

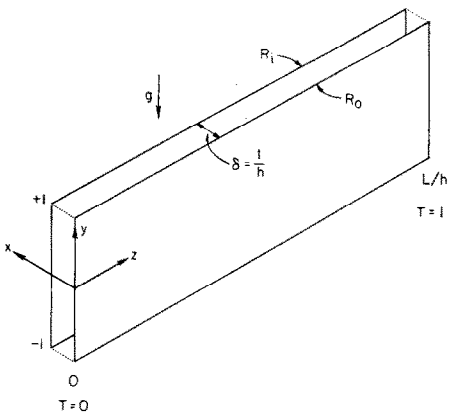

FIG. 5. Horizontal channel bounded by two vertical plates with different end temperatures.

the box is closed at the top and bottom, the velocity is zero at $y = \pm 1$. Consequently, expression (31) overestimates the axial velocity near the top and bottom walls, over vertical distances of the order of t.

The temperature distribution is

$$T = K_1 z + K_2 + \tfrac{1}{8} K_1^2 Ray F_T(x), \tag{35}$$

where $F_T(x)$ depends on the conducting properties of the two vertical walls. For the extreme cases illustrated in Fig. 4, F_T assumes the following simpler forms:

$$F_T = \tfrac{11}{24}\delta^2, \quad \text{both walls insulated,} \tag{36}$$

$$F_T = \tfrac{1}{3}(\delta^3 x - 2\delta x^3 + x^4), \quad \text{both walls isothermal,} \tag{37}$$

$$F_T = \tfrac{1}{3}(\delta^4 - 2\delta x^3 + x^4), \quad \text{one wall insulated, the other isothermal.} \tag{38}$$

These findings agree qualitatively with the isothermal patterns shown in Fig. 3 for $\rho = 0.8$.

Expressions (31) and (35) can finally be used to estimate the Nusselt number for axial heat transfer through the box shown in Fig. 5. The method follows identically the steps outlined in the preceding section and is not repeated here.

SPACE FILLED WITH POROUS MEDIUM

We will now examine the horizontal counterflow induced by different end temperatures when the annular space of Fig. 1 is filled with a porous medium. The permeability K is assumed uniform, independent of orientation. The medium is saturated with a quasi-incompressible fluid which obeys the Boussinesq approximation, equation (8). The horizontal cylindrical surfaces are impermeable conducting sheets characterized by resistances R_i, R_o defined in equations (12a,b).

As in the preceding section, the heat transfer between the annular space and its environment is assumed negligible, except over the two end plates maintained at constant but different temperatures.

(a) *Formulation of the problem*

The analysis leading to expressions for the velocity, temperature and Nusselt number in the annular space follows the procedure presented in the preceding section. For this reason, many details will be skipped allowing us to focus on features characteristic to natural convection through porous media.

Assuming that Darcy's law applies, i.e. the Reynolds number based on pore diameter is less than one [8], the continuity, momentum and energy equations are

$$\frac{u}{r} + \frac{\partial u}{\partial r} + \frac{1}{r}\frac{\partial v}{\partial \theta} + \frac{\partial w}{\partial z} = 0, \tag{39}$$

$$u = -\frac{\partial P}{\partial r} + RaT\sin\theta, \tag{40a}$$

$$v = -\frac{1}{r}\frac{\partial P}{\partial \theta} + RaT\cos\theta, \tag{40b}$$

$$w = -\frac{\partial P}{\partial z}, \tag{40c}$$

$$u\frac{\partial T}{\partial r} + \frac{v}{r}\frac{\partial T}{\partial \theta} + w\frac{\partial T}{\partial z} = \nabla^2 T. \tag{41}$$

The dimensionless variables appearing in the above equation, r, z, u, v, w, T and P have been defined in equations (4)–(7). The Rayleigh number for this problem contains the permeability K,

$$Ra = \frac{g\beta r_o K \Delta T}{\alpha \nu}. \tag{42}$$

We are again interested in the natural convection pattern in the core region, i.e. away from the two ends. The boundary conditions throughout the core region are expressed in equations (10), (11).

(b) *The perturbation method*

Eliminating the pressure terms between the three momentum equations yields

$$\frac{\partial u}{\partial \theta} - \frac{\partial}{\partial r}(rv) = Ra\left[\sin\theta\frac{\partial T}{\partial \theta} - r\cos\theta\frac{\partial T}{\partial r}\right], \tag{43}$$

$$-\frac{\partial w}{\partial r} = Ra\sin\theta\frac{\partial T}{\partial z}. \tag{44}$$

The power series in Ra, expressions (15), are substituted into equations (39), (41), (43) and (44). Collecting the terms multiplying the same power of Ra provides the necessary set of equations for determining the successive corrections to the velocity and temperature field in the core region. The result is:

zeroth order

$$(u, v, w)_0 = 0, \tag{45}$$

$$T_0 = K_1 z + K_2; \tag{46}$$

first order

$$(u, v)_1 = 0, \tag{47}$$

$$w_1 = -K_1 r\sin\theta; \tag{48}$$

$$T_1 = K_1^2 \sin\theta\left(c_{-1}\frac{1}{r} + c_1 r - \frac{1}{8}r^3\right); \tag{49}$$

second order

$$(w, T)_2 = 0, \tag{50}$$

$$u_2 = K_1^2 \cos 2\theta f_u(r), \tag{51}$$

$$v_2 = K_1^2 \sin 2\theta f_v(r). \tag{52}$$

Coefficients c_{-1}, c_1 appearing in equation (49) depend on ρ, R_i, R_o and are determined by applying the temperature boundary conditions (11a,b). Functions f_u, f_v describing the secondary flow can be determined by solving the ordinary differential equations obtained from substituting u_2, v_2 into equations (43) and (44). However, of the perturbation solution presented above only the zeroth

and first order approximation contribute to the axial heat transport through the annular porous medium.

As a first approximation, the axial temperature gradient constant K_1 equals r_o/L. This value is expected to decrease steadily as Ra increases, depending also on whether the two end plates are permeable or not.

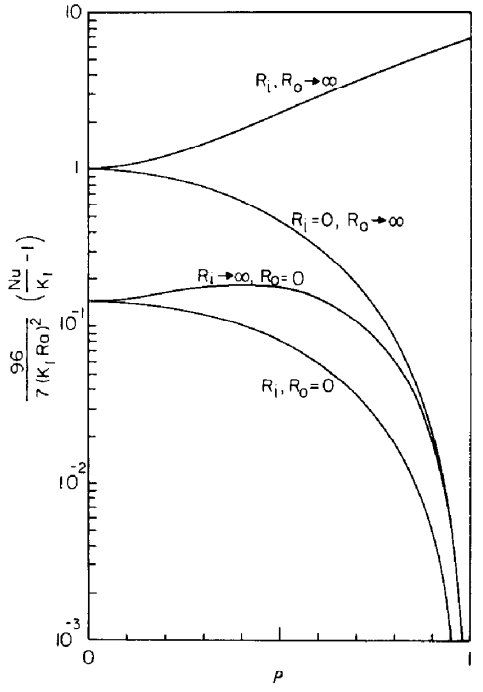

FIG. 6. Nusselt number vs radii ratio ρ for horizontal annular space filled with saturated porous medium.

(c) *Axial heat-transfer rate*

The Nusselt number for axial heat transport was defined in equation (27). Substituting the perturbation solution for w and T into equation (28) yields

$$Nu = K_1 + K_1^3 Ra^2 [\tfrac{1}{2}c_{-1} + \tfrac{1}{4}(1+\rho^2)c_1 - \tfrac{1}{48}(1+\rho^2+\rho^4)]. \quad (53)$$

As mentioned previously, c_{-1} and c_1 depend on the wall resistance parameters R_i, R_o. Figure 6 shows the variation of Nu with the radii ratio ρ in four extreme cases regarding the conducting properties of the concentric cylinders. As reference we used the case of a round pipe ($\rho = 0$) with non-conducting wall, for which the Nusselt number becomes

$$Nu = K_1 + \tfrac{7}{96}K_1^3 Ra^2. \quad (54)$$

Comparing Fig. 6 with Fig. 4 we observe that, as $r_i \to r_o$, the Nusselt number for the porous medium does not decrease as abruptly as for an annular space filled with incompressible fluid. There is a reason for this, namely, the narrowing of the annular space has no effect on the first order axial velocity which is independent of the shape of the vertical cross-section [see equation (48)]. If both cylindrical walls are non-conducting (R_i, $R_o \to \infty$), the Nusselt number increases as $\rho \to 1$; however, the axial heat-transfer rate Q decreases on account of the decreasing cross-sectional area, equation (27).

(d) *Horizontal counterflow between two vertical plates*

We conclude the study of natural convection through a horizontal annular space filled with porous material by making again the observation that the perturbation solution derived in (b) above contains information relevant to the parallel plate geometry sketched in Fig. 5. Applying the calculus of limits as $\rho \to 1$ and using transformations (32) and (33) we obtain the following expressions for the axial velocity and temperature pattern in a horizontal porous layer of rectangular cross-section ($h \gg t$):

$$w = -K_1 Ray, \quad (55)$$

$$T = K_1 z + K_2 + K_1^2 Ray f_T(x). \quad (56)$$

As before, h replaces r_o as a length scaling factor in the definitions of w, z, y, x and Ra. Function $f_T(x)$ depends on c_{-1}, c_1 as shown in expression (49). In the three limiting circumstances singled out throughout this study, f_T is

$$f_T = 1 - \tfrac{3}{2}\delta + \tfrac{3}{4}\delta^2 \cong 1,$$

both walls insulated, (57)

$$f_T = \tfrac{1}{2}x(\delta - x),$$

both walls isothermal, (58)

$$f_T = \tfrac{1}{2}(\delta^2 - x^2),$$

one wall insulated, the other isothermal, (59)

where $\delta = t/h$. One can finally combine equations (55) and (56) to estimate the net heat-transfer rate in the horizontal direction through the porous layer. The Nusselt number will depend on three parameters, Ra, t/h and K_1 (or h/L).

CONCLUDING REMARKS

In order to understand the mechanism of natural convection heat transfer in long horizontal spaces with different end temperatures, we studied analytically the natural counterflow in a space of annular cross section. Two situations have been considered, the case when the annular space is filled with an incompressible fluid and the case when the space is filled with a porous material saturated with an incompressible fluid.

In both cases, perturbation analyses in the Rayleigh number led to expressions for the velocity and temperature distributions in the middle portion of the annular space. This is the core region situated at some distance away from the two ends. The primary flow caused by the different end temperatures consists of two horizontal streams in counter current flow, the warmer branch flowing towards the cold end through the upper half of the cross-section. The velocity and temperature field in the core region is similar to the one found in horizontal round pipes [1–3] and flat ducts ($h \ll t$) [3–7].

The Nusselt number for axial heat transfer was shown to depend on the Rayleigh number (Ra) plus two geometrical parameters, the radii ratio (ρ) and the axial temperature gradient constant (K_1). The Nusselt number increases as both Ra and K_1 increase. It was shown that the axial heat-transfer rate decreases as one or both cylindrical walls become more conducting.

The solution for convection in a horizontal annular space was placed in the limit $r_i \to r_o$ to obtain closed form expressions for velocity and temperature between two vertical walls exposed horizontally to a finite temperature difference. The natural convection pattern in the geometry of Fig. 5 was shown to depend on the Rayleigh number based on the vertical dimension (h), the axial temperature gradient K_1 (of the order of h/L) and the cross-section aspect ratio t/h. The vertical wall thermal conductance was shown to be an effective means of reducing the axial heat-transfer rate through the horizontal space.

It is worth commenting on the axial temperature gradient constant K_1 which is a crucial element of the natural convection pattern discussed in this study. If the horizontal space is long ($r_o/L \ll 1$ or $h/L \ll 1$) the core region fills almost the entire space. If the Rayleigh number is moderate so that at any z the temperature difference between the upper (warm) stream and the lower (cold) stream is considerably smaller than the end-to-end ΔT, the zeroth order contribution $T_0(z)$ dominates the core temperature distribution. Under these circumstances the solid body conduction values for K_1, K_2 shown in expression (18) are adequate.

As the Rayleigh number increases, the temperature difference at any z increases causing a decrease in the bulk temperature gradient K_1. We can no longer assume, as in what led to equation (18), that $T = 0$ at $z = 0$ and $T = 1$ at $z = L/r_o$ since, at any z, the temperature varies considerably across the annular cross-section. The functions K_1 (Ra, L/r_o) and K_2 (Ra, L/r_o) can only be determined by solving the Navier–Stokes equations in the two end regions and matching the solution with the core solution presented in this study.

There are certain ways in which an end solution can be found. Studying the flow in horizontal rectangular cavities (flat ducts, $h \ll t$), Cormack *et al.* [4] developed a perturbation solution in h/L for the flow around a square end. The solution, however, is prohibitively complex to be carried out analytically. A much more expedient analytical method was employed by Bejan and Tien [7] for the flow in the two end regions of the horizontal cavity studied by Cormack *et al.* [4, 5] and Imberger [6]. The method consists of integrating the momentum and energy equations in the two end regions, using velocity and temperature profiles matching the core solution at the imaginary cross-sections where the end regions and the core region come in contact. The momentum and energy integral conditions prevailing in the two end regions provide the necessary information for estimating the unknown constants K_1 and K_2, once Ra and the aspect ratio h/L are specified. The integral method is quite flexible as shown by the authors who have also applied it to the flow through an open end (horizontal flat duct communicating with a large reservoir) [9] and to the flow near the end wall (permeable and impermeable) of a porous medium bounded by a horizontal cylinder [3].

An even simpler method which allows one to estimate the first correction in Ra and L/r_o beyond the zeroth order solution for K_1, K_2 of equation (18) is the pinned-core-solution approximation [7]. According to this method, even when the temperature varies across the annulus, the coldest point in the $z = 0$ cross-section approaches $T = 0$, whereas the warmest point at $z = L/r_o$ approaches $T = 1$. As shown in Fig. 3, depending on ρ, R_i, R_o, the temperature varies appreciably across the annulus. However, once ρ, R_i, R_o are specified, expressions (23), (35), (49) and (56) may be used to locate the points where the cross-section temperature is minimum and maximum. Undoubtedly, the two points lie on the vertical diameter, the coldest in the lower half at $\theta = -\pi/2$ and the warmest at $\theta = \pi/2$. Then, writing

$$T_{\min, z=0} = 0, \tag{60}$$

$$T_{\max, z=L/r_o} = 1, \tag{61}$$

corresponds to pinning the core solution to the externally imposed temperature difference. Equations (60) and (61) provide a system for determining K_1 and K_2 as functions of Ra and L/r_o. In the $Ra \to 0$ limit these findings will be identical to expression (18).

It is appropriate to conclude this discussion with a comment regarding the domain in which the asymptotic results developed in this study are valid. From the mathematical formulation of the problem, the theory is strictly valid in the limit $Ra \to 0$. Due to the algebraic complexity of the series solutions provided by the perturbation analysis in Ra small, only the first convective terms of two solutions (incompressible fluid, saturated porous medium) were derived. An approximate upper bound to the Rayleigh number for which the asymptotic solution applies can be obtained from the condition that the convective term must never exceed the conductive contribution in the make-up of the Nusselt number, equations (30) and (54). Thus, on an order of magnitude basis, we find

$$O(RaK_1) < 152, \text{ for incompressible fluid,} \tag{62}$$

$$O(RaK_1) < 3.7, \text{ for porous medium.} \tag{63}$$

Since in the conduction dominated regime the axial temperature gradient parameter K_1 is of order r_o/L, equation (18), criterion (62, 63), is expressed solely in terms of a modified Rayleigh number based on the physical gradient $\Delta T/L$, namely $Ra r_o/L$. This observation suggests that the asymptotic results presented

in this article are also applicable in the limit $r_o/L \to 0$ with Ra arbitrary but finite, such that the product $Ra r_o/L$ obeys criterion (62, 63).

Acknowledgement—The authors thank Professor J. Imberger of the Civil Engineering Department, University of California, Berkeley, for many valuable comments. This work was supported in part by a post doctoral fellowship awarded during 1976–1978 to A. Bejan by the *Miller Institute for Basic Research in Science*, University of California, Berkeley.

REFERENCES

1. S. W. Hong, Natural circulation in horizontal pipes, *Int. J. Heat Mass Transfer* **20**, 685–691 (1977).
2. A. Bejan and C. L. Tien, Fully developed natural counterflow in a long horizontal pipe with different end temperatures, *Int. J. Heat Mass Transfer* **21**, 701–708 (1978).
3. A. Bejan and C. L. Tien, Natural convection in a horizontal porous medium subjected to an end-to-end temperature difference, *J. Heat Transfer* **100**, 191–198 (1978).
4. D. E. Cormack, L. G. Leal and J. Imberger, Natural convection in a shallow cavity with differentially heated end walls. Part 1. Asymptotic theory, *J. Fluid Mech.* **65**, 209 (1974).
5. D. E. Cormack, L. G. Leal and J. H. Seinfeld, Natural convection in a shallow cavity with differentially heated end walls. Part 2. Numerical solutions, *J. Fluid Mech.* **65**, 231 (1974).
6. J. Imberger, Natural convection in a shallow cavity with differentially heated end walls. Part 3. Experimental results, *J. Fluid Mech.* **65**, 247 (1974).
7. A. Bejan and C. L. Tien, Laminar natural convection heat transfer in a horizontal cavity with different end temperatures, *J. Heat Transfer* **100**, 641–647 (1978).
8. M. Muskat, *The Flow of Homogeneous Fluids Through Porous Media*. J. W. Edwards, Michigan (1946).
9. A. Bejan and C. L. Tien, Laminar free convection heat transfer through horizontal duct connecting two fluid reservoirs at different temperatures, *J. Heat Transfer* **100**, 725–727 (1978).

CONVECTION NATURELLE DANS UN ESPACE HORIZONTAL LIMITE PAR DEUX CYLINDRES CONCENTRIQUES AVEC DIFFERENTES TEMPERATURES AUX EXTREMITES

Résumé—On étudie analytiquement l'écoulement de convection naturelle dans un long espace horizontal à section droite annulaire, isolé latéralement et avec les deux extrémités maintenues à différentes températures. Les distributions de vitesse et de température dans la portion centrale du volume sont déterminées par une analyse de perturbation en nombre de Rayleigh. Le nombre de Nusselt pour le transfert axial de chaleur dépend du nombre de Rayleigh, les deux rapports de forme r_i/r_0 et L/r_0 (rayon intérieur/rayon externe et longueur/rayon externe) et aussi des propriétés conductrices des deux parois cylindriques. On considère le cas où le volume est rempli par un fluide incompressible et le cas où il est rempli par un matériau poreux saturé par un fluide incompressible. La limite $r_i \to r_0$ est considérée pour obtenir des expressions correspondent au champs de vitesse et de température entre deux plans verticaux soumis à une différence de température dans la direction horizontale parallèle aux plans.

FREIE KONVEKTION IN EINEM WAAGERECHTEN RAUM, DER DURCH ZWEI KONZENTRISCHE ZYLINDER MIT UNTERSCHIEDLICHEN ENDTEMPERATUREN BEGRENZT IST

Zusammenfassung—Es wurde eine analytische Untersuchung der durch die Schwerkraft induzierten Strömung in einem langen, waagerechten Raum mit ringförmigem Querschnitt durchgeführt. Der Raum ist seitlich isoliert und wird an beiden Enden auf unterschiedlichen Temperaturen gehalten. Die Geschwindigkeits- und Temperaturverteilung im mittleren Teil des Raumes wurde aus einer Störungsanalyse mit der Rayleigh–Zahl abgeleitet. Es zeigte sich, daß die Nusselt–Zahl für den axialen Wärmetransport von folgenden Parametern abhing: der Rayleigh–Zahl, den Seitenverhältnissen r_i/r_0 und L/r_0 (innerer Radius/äußerer Radius und Länge/äußerer Radius) und von den Leitungseigenschaften der zwei zylindrischen Wände. Die Untersuchung wurde den Fall durchgeführt, bei dem der waagerechte Raum von einem inkompressiblen Fluid erfüllt ist, und für den Fall, bei dem der Raum von einem porösen, mit einem inkompressiblen Fluid gesättigten Material erfüllt ist. Schließlich wurde der Grenzfall $r_i \to r_0$ benutzt, um Beziehungen für die Strömung und die Temperaturverteilung zwischen zwei senkrechten Platten abzuleiten, bei denen eine endliche Temperaturdifferenz in waagerechter Richtung, parallel zu den Platten, vorleigt.

ЕСТЕСТВЕННАЯ КОНВЕКЦИЯ В ГОРИЗОНТАЛЬНОЙ ОБЛАСТИ, ОГРАНИЧЕННОЙ ДВУМЯ КОНЦЕНТРИЧЕСКИМИ ЦИЛИНДРАМИ С РАЗЛИЧНЫМИ ТЕМПЕРАТУРАМИ НА ТОРЦАХ

Аннотация — Проведено аналитическое исследование течения, вызываемого силами тяжести, в длинном горизонтальном изолированном кольцевом канале с различными температурами на торцах. С помощью метода возмущений по числу Релея получено распределение скорости и температуры в центральной части канала. Показано, что число Нуссельта для аксиального переноса тепла зависит от числа Релея, величины отношения внутреннего радиуса r_i к внешнему радиусу r_0 и отношения длины L к внешнему радиусу r_0, а также от теплопроводности стенок цилиндров. Анализ проведен для случая, когда горизонтальный канал заполнен несжимаемой жидкостью, и случая, когда канал заполнен пористым материалом, насыщенным несжимаемой жидкостью. Наконец, при выводе выражений для полей течения и температуры между торцами цилиндров при наличии суммарной разности температур в горизонтальном направлении, параллельном торцам, использовался предел $r_i \to r_0$.